THE ASTROPHYSICAL JOURNAL, 433:29–38, 1994 September 20

LUMINOSITY FUNCTIONS OF BL LACERTAE OBJECTS

ANNA WOLTER,[1] ALESSANDRO CACCIANIGA,[1] ROBERTO DELLA CECA,[2] AND TOMMASO MACCACARO[1]
Received 1993 August 23; accepted 1994 March 28

ABSTRACT

We derive here the luminosity functions in the radio, X-ray, and, for the *first time*, optical band, of two complete samples of BL Lac objects. The samples analyzed are the only sizable samples currently available with a reasonably complete flux and redshift information and are derived from X-ray selection (XBL; 30 objects from the Extended Medium-Sensitivity Survey (EMSS) sample) and radio selection (RBL; 34 objects from the 1 Jy sample).

We study the evolution properties of the XBL sample and find a negative evolution of the X-ray luminosity function [$L_X(z) \sim L_X(0)e^{-7.0\tau}$] consistent, albeit less dramatic, with previous findings from a smaller EMSS-derived sample (Morris et al. 1991). The RBL sample, instead, shows a marginal positive evolution in the radio band (Stickel et al. 1991). We then derive the evolution parameters and compute the de-evolved luminosity function for the two samples in the three bands (radio, optical, and X-ray). From the comparison of luminosity functions we find that XBLs outnumber RBLs in the optical and X-ray band, but they are found in consistent numbers, but at lower luminosities, in the radio band. These results are in agreement with models like the wide jet model (Celotti et al. 1993); however, the different evolution parameter and the sign of evolution for the two samples have yet to be understood and explained theoretically.

A density of ~ 20 BL Lac objects per steradian at $m_V = 17$ is derived from the integration of the XBL optical luminosity function. We find that the negative results obtained by current polarization and color surveys are consistent with our results and with the properties of BL Lac objects. New search techniques have to be devised in order to create sizable samples of *optically* selected BL Lac objects.

Subject headings: BL Lacertae objects: general — radio continuum: galaxies — X-rays: galaxies

1. INTRODUCTION

BL Lac objects are among the most elusive and enigmatic class of extragalactic objects. They are defined by rapid variability, high luminosity, relatively high optical polarization, and an optical continuum with weak or absent emission lines. Although studied extensively for more than 15 years, only approximately 150 BL Lac objects are known up to now. By comparison, several thousand quasars are known.

The observed properties of BL Lac objects have been explained in terms of relativistic beaming. In this scenario, originally proposed by Blandford & Rees (1978), these objects are characterized by Doppler-boosted and beamed radiation arising from a line-of-sight bulk relativistic motion of an emitting plasma. This hypothesis, however, opens a new question about the nature of the "parent population," i.e., the class of astronomical objects intrinsically identical to BL Lac objects but pointed away from us. This topic has been extensively discussed in the literature in the last few years (Padovani & Urry 1990, 1991, 1992; Urry, Padovani, & Stickel 1991; Stickel et al. 1991; Padovani 1992; Celotti et al. 1993), and there is now evidence that the most likely candidates for the parent population of most BL Lac objects are Fanaroff-Riley (F-R) type I radio galaxies.

One of the fundamental tests of the relativistic beaming hypothesis is the prediction of the cosmological properties (e.g., the luminosity function [LF] and cosmological evolution in different energy bands) of BL Lac objects as compared with those of the parent population. This comparison requires sizable, statistically complete samples of objects. However, it is not easy to create statistically complete samples of BL Lac objects. Because of their featureless optical spectra, BL Lac objects cannot be easily found in objective prism surveys which are used to search for distant quasars. Grism surveys could detect high-redshift BL Lac objects with large breaks in their spectra (e.g., Lyα absorption; Schneider, Schmidt, & Gunn 1991), but so far none have been discovered in this way. Not all BL Lac objects exhibit the strong UV excess seen in quasars; thus, color selection is not so efficient in finding them. Up to now, optical color surveys for quasars have found very few BL Lac objects (e.g., Green, Schmidt, & Liebert 1986; Fleming et al. 1993), and optical polarization surveys have failed to find any confirmed ones (see, e.g., Jannuzi, Green, & French 1993a). Only a few BL Lacs have been found as a consequence of their optical variability (Hawkins et al. 1991).

X-ray and radio observations, on the other hand, have proven to be an efficient way to create sizable samples of BL Lac objects suitable for statistical studies, and in fact most of the known ones have been discovered in this way. However, X-ray and radio selection seems to find two classes of BL Lacs (XBL and RBL) that are different in their global properties. XBLs, if compared with RBLs, show a lesser amount of optical variability in total and polarized light (Jannuzi 1990; Stocke et al. 1989), a larger starlight fraction in their optical spectra (Morris et al. 1991), a polarization percentage smaller in amplitude and often constant in position angle (Jannuzi 1990; Jannuzi et al., 1993b), and a smaller core-to-extended radio flux ratio (Perlman & Stocke 1993).

On the basis of these observed differences many authors (e.g., Stocke et al. 1985; Maraschi et al. 1986) have suggested that XBLs and RBLs are similar objects which are viewed at different angles with respect to the radio and optical beaming axis and in which the X-ray beams are broader than the radio and optical beams. If the proposed unification scheme is

[1] Osservatorio Astronomico di Brera, via Brera 28, 20121 Milano, Italy.
[2] Johns Hopkins University, Baltimore, MD 21218.

correct, then XBL should be the intermediate class between RBL and F-R I radio galaxies.

It is thus interesting to study these two classes of objects separately and to compare their respective properties.

Over the past few years, statistically complete samples of both XBLs (Gioia et al. 1990) and RBLs (Stickel et al. 1991) have become available. Other authors have recently compared the correlations between luminosities in different bands (Padovani 1992) and the radio (Perlman & Stocke 1993; Laurent-Muehleisen et al. 1993) and infrared (Gear 1993) properties for XBL and RBL.

In this paper we concentrate on the comparison of the LF and cosmological evolution of RBLs and XBLs in the radio, optical and X-ray bands, which is an important tool to test the proposed unification scheme and constrain the details of the beaming model.

The paper is organized as follows: we discuss the complete samples we use in § 2. In § 3 we present the method used, the resulting evolution of the samples, and the LFs in the three bands. In § 4 we compare the LF of the two samples in the three bands, and with theoretical predictions, we estimate the optical counts of BL Lac objects and address the problem of the "recognition" of low-luminosity BL Lac objects. Our conclusions are summarized in § 5.

Throughout the paper, a Hubble constant $H_0 = 50$ km s^{-1} Mpc^{-1} and a Friedmann universe with a deceleration parameter $q_0 = 0$ are assumed.

2. THE SAMPLES

To derive and study the LF of a class of astronomical objects, statistically complete samples of objects that represent the properties of the entire population are needed. Here we use the X-ray sample from the Extended Medium-Sensitivity Survey (EMSS) (Gioia et al. 1990) to derive a complete sample of X-ray–selected BL Lac objects (XBLs), and the complete sample of radio-selected BL Lac objects (RBL) from the 1 Jy radio sample (Stickel et al. 1991). Since X-ray, optical, and radio data exist for virtually all the objects in these samples, we can compute the LF in the three bands.

Variability at all wavelengths is one of the main characteristics of BL Lac objects. For the RBL sample, where possible, mean fluxes are given (see discussion in Padovani 1992). However, we note that, for most objects in the XBL sample, we possess only single epoch measurements, and observations in different bands were performed at different times, often several years apart. We use these data with the caution that variability might somewhat affect both the relationships between the luminosities in the various bands (see § 3.2) and the derivation of the LF. We believe, however, that the uncertainties thus introduced are not significant given the overall scatter in the observed quantities.

2.1. *The XBL Sample*

The EMSS is described in detail in Gioia et al. (1990). The optical identification criteria and their results are presented in Stocke et al. (1991). The selection criteria for classification of an EMSS source as a BL Lac object, given in Stocke et al. (1991) and discussed in detail in Morris et al. (1991), are summarized here:

1. Equivalent width of any emission line less than 5 Å;
2. Evidence for the presence of a nonthermal continuum, given by a Ca II break smaller than 25% in the identification spectra.

TABLE 1

THE *EXTENDED* EMSS SAMPLE OF BL LAC OBJECTS

Name	z	f_X[a]	f_R[b]	f_O[c]
MS 0122.1+0903.....	0.339	0.12	1.4	0.04
MS 0158.5+0019.....	0.299	1.46	11.3	0.24
MS 0205.7+3509.....	0.318	0.09	3.6	0.07
MS 0257.9+3429.....	0.245	0.20	10.0	0.14
MS 0317.0+1834.....	0.190	2.08	17.0	0.20
MS 0419.3+1943.....	0.512	0.42	8.0	0.03
MS 0607.9+7108.....	0.267	0.21	18.2	0.05
MS 0737.9+7441.....	0.315	1.64	24.0	0.64
MS 0922.9+7459.....	0.638	0.18	3.3	0.05
MS 0950.9+4929.....	>0.6	0.35	3.3	0.07
MS 0958.9+2102.....	0.344	0.03	1.5	0.04
MS 1133.7+1618.....	...	0.06	9.0	0.04
MS 1207.9+3945.....	0.615	0.25	5.8	0.08
MS 1221.8+2452.....	0.218	0.20	26.4	0.31
MS 1229.2+6430.....	0.164	0.56	42.0	0.64
MS 1235.4+6315.....	0.297	0.31	7.0	0.13
MS 1256.3+0151.....	...	0.04	8.0	0.03
MS 1258.4+6401.....	...	0.07	12.0	0.03
MS 1402.3+0416.....	0.200	0.18	20.8	0.54
MS 1407.9+5954.....	0.495	0.33	16.5	0.05
MS 1443.5+6349.....	0.299	0.26	11.6	0.05
MS 1458.8+2249.....	0.235	0.18	29.8	0.70
MS 1534.8+0148.....	0.312	0.34	34.0	0.12
MS 1552.1+2020.....	0.222	0.72	37.5	0.30
MS 1704.9+6046.....	0.280	0.08	1.8	0.08
MS 1757.7+7034.....	0.407	0.39	7.2	0.18
MS 2143.4+0704.....	0.237	0.37	50.0	0.22
MS 2336.5+0517.....	...	0.08	4.9	0.03
MS 2342.7−1531.....	...	0.08	2.3	0.08
MS 2347.4+1924.....	0.515	0.08	3.2	0.02

[a] Monochromatic X-ray flux at 1 keV in μJy.
[b] Monochromatic radio flux at 5 GHz in mJy.
[c] Monochromatic optical flux at 5500 Å in mJy.

Morris et al. (1991) used a subsample of the EMSS, constrained in flux ($S_X \geq 5 \times 10^{-13}$ ergs cm^{-2} s^{-1}) and declination of the sources ($\delta \geq -20°$), to define an XBL *complete* sample of 22 objects with full redshift information. To improve upon the statistics, we seek to use a larger sample than in Morris et al. (1991). We choose a flux limit of 2×10^{-13} ergs cm^{-1} s^{-1}, and the same declination limit.[3] The sample thus defined contains 567 sources, out of which 30 are BL Lac objects. Only one source (MS 2136.1−1509) in this sample is not identified.[4] The unidentified source has been observed at 6 cm with the VLA[5] (C configuration) and has not been detected (3 σ upper limit of $\sim$0.6 mJy). Following the conclusion of Stocke et al. (1990) that no radio-quiet XBL exists, we are justified in assuming that this source is not a BL Lac object. We can thus consider this *extended* sample, which contains 30 objects, eight more than the sample of Morris et al. (1991), as statistically complete and unbiased (see the discussion in § 3.3 of Morris et al. 1991), suitable for statistical analysis.

In Table 1 we report all the information for the XBL sample. For one object (MS 0950.9+4929) new measurements reported in Perlman & Stocke (1993) indicate a lower limit $z \geq 0.6$ from

[3] The sky coverage for this subsample of the EMSS, computed assuming an energy spectral index $\alpha_x = 1.0$, is reported in Fig. 5 (*solid line*). Fluxes (0.3–3.5 keV) have been corrected for absorption using the measured Galactic hydrogen column density along the line of sight to each source.

[4] In the Stocke et al. (1991) paper there are two sources that satisfy our selection criteria and are unidentified. Now the first one, MS 1610.4+6616, has been identified with a distant cluster of galaxies (Gioia & Luppino 1994).

[5] The Very Large Array (VLA) is a facility of the National Radio Astronomy Observatory (NRAO), which is operated by Associated Universities, Inc., under cooperative agreement with the National Science Foundation.

the optical image of the source. We have converted the (0.3–3.5) keV fluxes to monochromatic fluxes at 1 keV assuming an energy spectral index of 1 (see Maccacaro et al. 1988). The V-magnitudes are converted to a monochromatic flux at 5500 Å using the formula

$$f_{5500\,\text{Å}}(\text{mJy}) = 10^{(-0.4\times m_V + 6.565)}.$$

Radio fluxes are given in mJy.

2.2. *The RBL Sample*

The 1 Jy catalog is described in detail in Kühr et al. (1981) and contains 518 objects detected at or above a flux limit of 1 Jy at 5 GHz. Stickel et al. (1991) discuss the extraction of a complete sample of BL Lacs from the 1 Jy catalog, using the criteria summarized below:

1. Flat or inverted radio specrum (energy index $\alpha \leq 0.5$ between 11 and 6 cm, $S(\nu) \propto \nu^{-\alpha}$);
2. V-magnitude of the optical counterpart greater than 20 to ensure that identifications are complete for the entire sample;
3. Weak emission lines, if at all present in the optical spectrum, with rest frame equivalent width $W_{\lambda,\text{rest}} \leq 5$ Å.

The resulting number of RBLs is 34, of which five lack X-ray information and eight have no measured redshift; for three of these a lower limit is given by faint absorption lines of probable cosmological origin, while for the remaining five a lower limit of $z = 0.2$ is implied by the pointlike optical image of the sources (Stickel et al. 1991). X-ray fluxes (in μJy) are taken from Padovani (1992) and one from Biermann et al. (1992). The redshift for PKS 0118 – 272 is taken from Falomo (1991).

In Table 2 we report redshifts, fluxes and magnitudes for the RBL sample. The optical monochromatic fluxes at 5000 Å reported in Padovani (1992) were converted to monochromatic fluxes at 5500 Å assuming an optical energy spectral index of 1.5, as in Padovani (1992). We note that the radio fluxes are here given in Jy.

TABLE 2

THE COMPLETE 1 Jy SAMPLE OF BL LAC OBJECTS

Name	z	f_X[a]	f_R[b]	f_O[c]
PKS 0048 – 097	>0.2	0.08	1.98	1.5
PKS 0118 – 272	0.559	0.2	1.14	1.6
PKS 0138 – 097	>0.501	1.5	1.22	0.2
PKS 0235 + 164	0.940	0.2	2.85	0.6
PKS 0426 – 380	>1.030	...	1.17	0.1
S5 0454 + 844	>0.2	0.06	1.39	0.5
PKS 0537 – 441	0.896	0.2	4.00	3.8
S5 0716 + 714	>0.2	4.6	1.12	7.0
PKS 0735 + 178	>0.424	0.3	1.99	2.5
S4 0814 + 425	(?)0.258	1.6	1.69	0.2
PKS 0820 + 225	0.951	...[d]	1.60	0.1
PKS 0823 + 033	0.506	0.3	1.32	0.5
S4 0828 + 493	0.548	2.8	1.03	0.1
PKS 0851 + 202	0.306	0.7	2.62	3.5
S4 0954 + 658	0.367	0.5	1.46	0.7
PKS 1144 – 379	1.048	...	1.61	0.5
B2 1147 + 245	>0.2	0.1	1.01	1.3
B2 1308 + 326	0.997	0.1	1.53	0.6
S4 1418 + 546	0.152	0.2	1.09	3.0
PKS 1514 – 241	0.049	0.6	2.00	4.3
PKS 1519 – 273	>0.2	...	2.35	0.2
PKS 1538 + 149	0.605	0.3	1.96	0.4
S4 1652 + 398	0.033	13.0	1.42	12.7
PKS 1749 + 096	0.320	0.4	1.87	0.5
S5 1749 + 701	0.770	1.9	1.08	0.7
S5 1803 + 784	0.684	0.2	2.62	0.8
S4 1807 + 698	0.051	1.2	2.26	7.0
S4 1823 + 568	0.664	1.7	1.66	0.1
PKS 2005 – 489	0.071	7.0	1.23	7.0
S5 2007 + 777	0.342	3.7	1.26	0.9
PKS 2131 – 021	(?)0.557	0.09	2.12	0.1
PKS 2200 + 420	0.069	2.00	4.77	4.2
PKS 2240 – 260	0.774	...	1.03	0.2
PKS 2254 + 074	0.190	0.08	1.19	1.0

[a] Monochromatic X-ray flux at 1 keV in μJy.
[b] Monochromatic radio flux at 5 GHz in Jy.
[c] Monochromatic optical flux at 5500 Å in mJy.
[d] Owing to a typographical error, the X-ray flux of 0828 + 493 had been erroneously assigned to 0829 + 225 in Padovani 1992—see Giommi & Padovani 1994.

3. THE LUMINOSITY FUNCTIONS

Having defined one complete sample of XBL and one of RBL, with virtually complete radio, optical and X-ray data, we can derive the luminosity functions for both samples in the three bands. It is relatively straightforward to determine the LF in the same band in which the sample has been selected. We will call this the "selection" band: it is the X-ray for XBLs and the radio for RBLs. The resulting LF will be indicated as sLF. The derivation of the LF in bands different from the selection band (we will call them generically the "nonselection" bands, i.e., optical and radio for XBL and optical and X-ray for RBL; the relative luminosity function will be indicated as $\bar{s}$LF) is more complex. To do this we have generalized the $1/V_a$ estimator method, taking into account the volumes in the selection band, to derive the corresponding volumes for the nonselection band. The application of the method to both cases is described in the next paragraph.

3.1. *The Method*

Our derivation of X-ray, radio, and optical luminosity functions is based on the method described in detail by Avni & Bahcall (1980) concerning the coherent analysis of a set of independent samples. It is based on the $1/V_a$ estimator, where V_a is the available volume, i.e., the volume within which an object could be detected above the flux limit(s) of the sample. It takes into account the amount of sky surveyed and the possibility of having different flux limits (see eq. [42] of Avni & Bahcall 1980). Through this procedure, we can obtain for each object an available volume, $V_{a,i}$, determined by its luminosity and the flux limits in the selection band. When the definition of the sample also includes a limit in a different band, as in the case of the 1 Jy sample of BL Lac objects ($m_v \leq 20$), V_a is computed using the most restrictive limit, i.e., using the smaller calculated $z_{\max}$ (see Maccacaro et al. 1991; Della Ceca et al. 1992 for an application of this method to derive the cosmological evolution properties of the EMSS active galactic nuclei [AGNs] sample.) We can divide the observed range of luminosities in a number of bins of equal logarithmic width. For the selection band the differential luminosity function in the jth bin of width ΔL_j is then the sum of volume densities over the objects in that bin, that is,

$$\Phi(L_j) = \frac{1}{\Delta L_j}\sum \frac{1}{V_{a,i}},$$

where L_j is the optical, radio, or X-ray luminosity in the center of the jth bin.

For the nonselection bands, we have a situation in which all the objects have been detected. The available volumes V_a are

essentially determined by the selection and are thus the same as for the selection band (X-ray for XBLs, and radio in conjunction with optical limits for RBLs). For this reason the differential $\bar{s}$LF is computed as the sLF, but using the volumes of the selection band and the luminosities in the nonselection band. We have also tested different choices of the starting point for the bin, and its relative position with respect to the first object in the distribution, and have found that all the resulting LF are consistent with each other.

We compute the errors taking into account the possible variation of the values of $1/V_a$. We note that the available volume V_a for each object is defined only by the flux limits in the selection band and does not take into account the limits in the other bands which do not define the sample. The error bars are then given by

$$\sigma_{\pm} = (\epsilon_{\pm} - N)\left(\frac{1}{N}\sum V_{a,i}^{-2}\right)^{1/2} \Big/ I ,$$

where $\epsilon_{\pm}$ are the Poissonian upper and lower limits (Gehrels 1986), N is the number of objects inside the bin, and I is the width of the bin under consideration (see also Marshall 1985). Since the volume is defined in the selection band, we expect a significant variation of the values of V_a inside a single bin in the calculation of a $\bar{s}$LF. The term $\sum V_{a,i}^{-2}$ weighs each observation by its contribution to the sum and becomes important when the volumes associated with the individual objects change significantly within a single bin, i.e., when calculating the $\bar{s}$LF.

We will apply this method to construct the LF for XBL and RBL in the three bands: X-ray, optical, and radio. However, since BL Lac objects have shown evidence of evolution of their properties with cosmic time (e.g., Morris et al. 1991; Stickel et al. 1991), we need to assess the evolution in each band, in order to combine the information for objects at different redshifts. We study here also the problem of deriving the evolution characteristics in the nonselection bands.

3.2. *The Evolution*

Evolution in the BL Lac object properties has been observed for both XBLs and RBLs in their respective selection bands. XBLs and RBLs show different evolutionary behaviors: for the X-ray selected BL Lac objects, Morris et al. (1991) found strong evidence that they were either fainter or less common per comoving volume at earlier times, i.e., they show a negative evolution with a $<1\%$ probability of a positive or zero evolution. On the contrary, the RBL show a slightly positive evolution consistent with the case of zero evolution (Stickel et al. 1991).

Since the *extended* sample of XBLs is now significantly larger than the *complete* sample used in Morris et al. (1991), we have performed the V_e/V_a analysis on the *extended* sample (see Morris (1991) for the detailed description of the procedure and the problems involved). We have found $\langle V_e/V_a\rangle = 0.36 \pm 0.05$, which confirms the existence of a negative evolution.[6] If we use a luminosity evolution of the form $L_X(z) = L_X(0)(1+z)^{\gamma}$, we find that the evolution computed for the XBLs is quite consistent with the findings of Morris et al. (1991) but a little less extreme ($\gamma = -4.9$). Furthermore, given the larger number of objects, the resulting 2 σ range on γ is smaller (-11.5, -0.9). For reference, Morris (1991) found $\gamma = -7.0$ and a 2 σ range of (-16.25, -1.5).

To compare the evolutionary properties of XBLs with those of RBLs we choose to test for a luminosity evolution (as used by Stickel et al. 1991) of the form $L_X(z) = L_X(0)\exp c\tau$, where τ is the look-back time. In this case the best-fit cosmological evolution parameter becomes $c_X = -7.0$ and a zero evolution case is ruled out at 2 σ confidence level (2 σ interval on c_X: -15.9, -1.3). The data do not allow us to give any preference for one or the other choice of evolutionary model. It would be interesting, when larger samples of BL Lac objects become available, to test if, as in the case of the X-ray selected AGNs (Della Ceca et al. 1992), a power-law evolution model is preferred over the exponential evolution model.

Finally, we have also implemented a method to estimate the evolution in the nonselection bands (i.e., the radio and optical band for the XBLs and the X-ray and optical band for the RBL). It is based on the following assumptions.

1. The evolution in the selection band is that found by us and by Stickel et al. (1991), respectively, for XBL and RBL.

XBL (this paper):

$$L_X(z) = L_X(0)\exp c_X\tau , \qquad c_X = -7.0 . \tag{1}$$

RBL (Stickel et al. 1991):

$$L_R(z) = L_R(0)\exp c'_R\tau , \qquad c'_R = 3.1 , \tag{2}$$

where τ is the look-back time.

2. The radio, optical and X-ray luminosities of a sample of objects are related by the general law (assumed independent from z and other properties):[7]

$$L_I \propto (L_J)^{\beta_{J,I}} , \tag{3}$$

where I and J are equal to O (optical band), R (radio band) or X (X-ray band).

With these assumptions the evolution in a "nonselection" band is given by

$$L_I(z) = L_I(0)\exp c_I\tau ,$$

with

$$c_I = c_X\beta_{X,I}$$

for the XBL and

$$c'_I = c'_R\beta_{R,I}$$

for the RBL.

We have then to derive the correlation between luminosities in the different bands. In Figure 1 we present two panels for XBLs (L_O vs. L_X, and L_R vs. L_X) and two for RBLs (L_O vs. L_R, and L_X vs. L_R).[8] For the five XBL without redshift, we extracted randomly fifty sets of five values from the observed XBL redshift distribution and combined the random sets with the observed redshifts to check how the correlation between luminosities changes as a function of this uncertainty. That is,

[6] The fact that five redshifts are unknown has only a negligible influence both on the resulting value of $\langle V_e/V_a\rangle$ and on the derived evolution parameters, as we tested imposing alternatively the highest and the smallest value for z to the five objects.

[7] To evaluate the assumption of nonevolving luminosity ratios, we divided the sample into two different redshift bins, and we find no evidence for different correlations at low and high z.

[8] L_R, L_O, and L_X are the monochromatic luminosities, at 5 GHz, 5500 Å, and 1 keV, respectively, multiplied by the relative frequency.

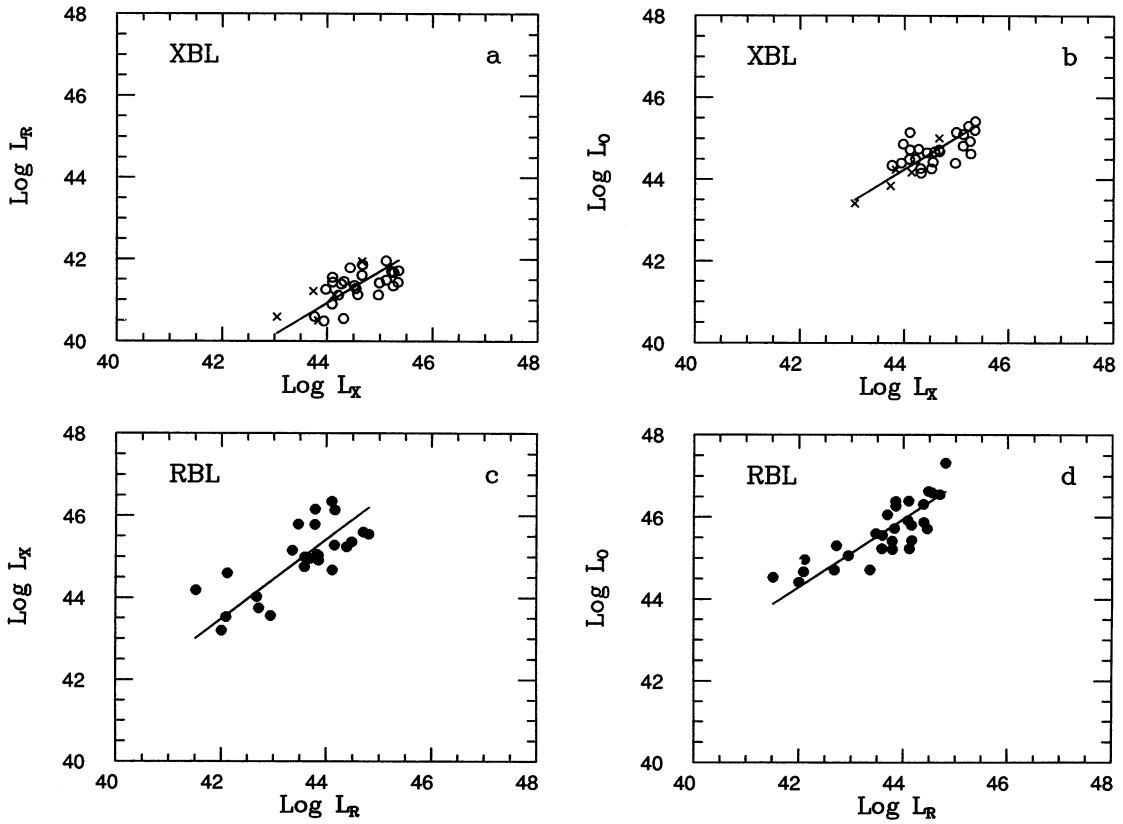

FIG. 1.—Luminosity-luminosity correlations for XBLs (*open circles*) and RBLs (*filled circles*). The fit is derived with the OLS method, as described in the text. We stress that, for XBLs, the lines represent the mean value of the correlations derived with the simulations (see text for details) and not a fit to the plotted data points. (*a*) L_R vs. L_X for XBLs; crosses indicate the 5 objects with "simulated" redshifts; (*b*) L_O vs. L_X for XBLs; crosses indicate the 5 objects with "simulated" redshifts; (*c*) L_X vs. L_R for RBLs; (*d*) L_O vs. L_R for RBLs.

we calculate a slope from a set of 30 objects, 25 with known redshift plus, in turn, each of the 50 sets with 5 randomly chosen redshifts. If we plot the histogram of the best-fit slopes thus derived for the correlation (see below for the details of the OLS bisector method used), we find that the dispersion is quite smaller than the statistical error associated to the correlation. To derive the fit, we thus assume the mean of the histogram as the value for the slope of the correlation, and the combination in quadrature of the dispersion and the statistical error for the uncertainty. For the purpose of deriving the XBL LFs, we have chosen one of these randomly extracted set of five values for the unknown redshifts. The set is such that it best represents the mean of the correlation slope distribution between X-ray and radio or optical luminosity (i.e., as discussed above, it falls nearest the peak of the two histograms). This set is also used to plot the points in Figure 1, in which the five BL Lac objects are indicated by a cross. For the RBL, there are 29 objects in the L_O versus L_R plot (we excluded the five objects without redshift), and 25 objects in the L_X versus L_R plot (we further excluded those sources without X-ray information). To estimate the values of $\beta_{J,I}$ we have computed the linear regressions of the logarithms of the luminosities involved. Since the intrinsic scatter of the data dominates the errors arising from the measurement process, and since our intent is to determine the underlying functional relationship between the two luminosities, we have chosen a method of linear regression that treats the data symmetrically, i.e., that does not depend on the choice of "independent" and "dependent" variables. We believe that the "ordinary least-squares fit bisector" (OLS bisector) described in detail in Isobe et al. (1990) is the best way of treating the data. In brief, the method finds the line that bisects the two ordinary least-squares fits of Y on X and of X on Y.

For the XBLs we find $\beta_{X,R} = 0.77 \pm 0.11$ with a correlation coefficient $r = 0.65$; $\beta_{X,O} = 0.78 \pm 0.06$ with a correlation coefficient $r = 0.74$. For the RBLs we find $\beta_{R,X} = 0.97 \pm 0.14$ with a correlation coefficient $r = 0.75$; $\beta_{R,O} = 0.83 \pm 0.09$ with a correlation coefficient $r = 0.82$. The level of significance of all the above correlations is $\geq 99\%$. We note that the correlation analyses done by Morris et al. (1991) and Padovani (1992) used different regression algorithms, so that the results and the correlation coefficients are not directly comparable. However, we agree with these results on the fact that the strongest correlation seen is the one between optical and radio luminosities. The resulting evolution parameters are listed in Table 3A for the XBLs and in Table 3B for the RBLs. The errors on the evolution parameters were computed on the basis of the uncertainty propagation, keeping account of the asymmetry of the 1 σ intervals.

3.3. *Resulting Luminosity Function*

1. *XBL.*—The differential LFs of the XBLs in the radio, optical, and X-ray bands are presented in Figure 2 (*open circles*). The best-fit evolution parameters (from Table 3A) have been used to de-evolve luminosities at $z = 0$. The LFs were derived using all the 30 objects of the sample, including the five

TABLE 3A

EVOLUTION PARAMETERS OF THE XBLs: $L(z) = L(0)\exp(c\tau)$

Parameter	Value	1 σ
c_X.....	−7.0	(−10.9, −3.9)
c_R.....	−5.4	(−8.5, −2.9)
c_O.....	−5.5	(−8.6, −3.0)

NOTES.—Evolution parameters of the XBLs assuming a luminosity evolution of the type $L(z) = L(0)\exp(c\tau)$. The value of the evolution parameter in the X-ray band is computed with the V_e/V_a method. The evolution parameters in the radio and optical bands are computed according to the method described in the text.

TABLE 3B

EVOLUTION PARAMETERS OF THE RBLs: $L(z) = L(0)\exp(c'\tau)$

Parameter	Value	1 σ
c'_X.....	3.0	(1.6, 4.2)
c'_R.....	3.1	(1.7, 4.2)
c'_O.....	2.6	(1.4, 3.6)

NOTES.—Evolution parameters of the RBLs assuming a luminosity evolution of the type $L(z) = L(0)\exp(c'\tau)$. The value of the evolution parameter in the radio band is from Stickel et al. 1991. The evolution parameters in the X-ray and optical bands are computed according to the method described in the text.

sources with unknown redshifts. We have used the lower limit on z for MS 0950.9+4929 as an actual estimate. To derive the LFs of XBLs, we have used the previously defined set (see § 3.2) of five z for the sources with unknown redshift. We have checked that the LFs are not very sensitive to the choice of redshift for these five objects, running a number of simulations from which we derive additional uncertainties (of the order of 20% or less for most of the bins, except for the one at the lowest luminosity for which the indetermination is higher) that are combined with statistical errors (computed as in § 3.1) for each bin. Therefore, we conclude that our results do not depend substantially on the assumptions made about the redshift of these objects. We applied a weighted least-squares fit to the LFs in the three bands. Results are presented in Table 4A. The radio and X-ray LFs can be well represented by a single power-law fit $[\Phi(L) = KL^{-B}]$ over the observed luminosity range. The fit of the optical LFs with a single power law is marginal, but the small number of points makes it unreasonable to test for a more complex form.

2. *RBL.*—The LFs of the RBL are shown in Figure 2 (*filled circles*). The best-fit evolution parameters (from Table 3B) have been used to de-evolve luminosities at $z = 0$. In the radio and in the optical band we have used all the 34 objects, including the five objects with unknown redshift, assuming a mean value of 0.56 and using the lower limits on z for the other three objects as actual estimates. In the X-ray band the LF was derived with the 29 objects with known X-ray flux. The X-ray LF was consequently normalized simply by reducing the sky coverage by a factor 29/34. Again, we apply a weighted least-squares fit assuming a single power-law fit $[\Phi(L) = KL^{-B'}]$. Results are listed in Table 4B. We have also evaluated the effect of our assumptions about the unknown redshifts by adopting

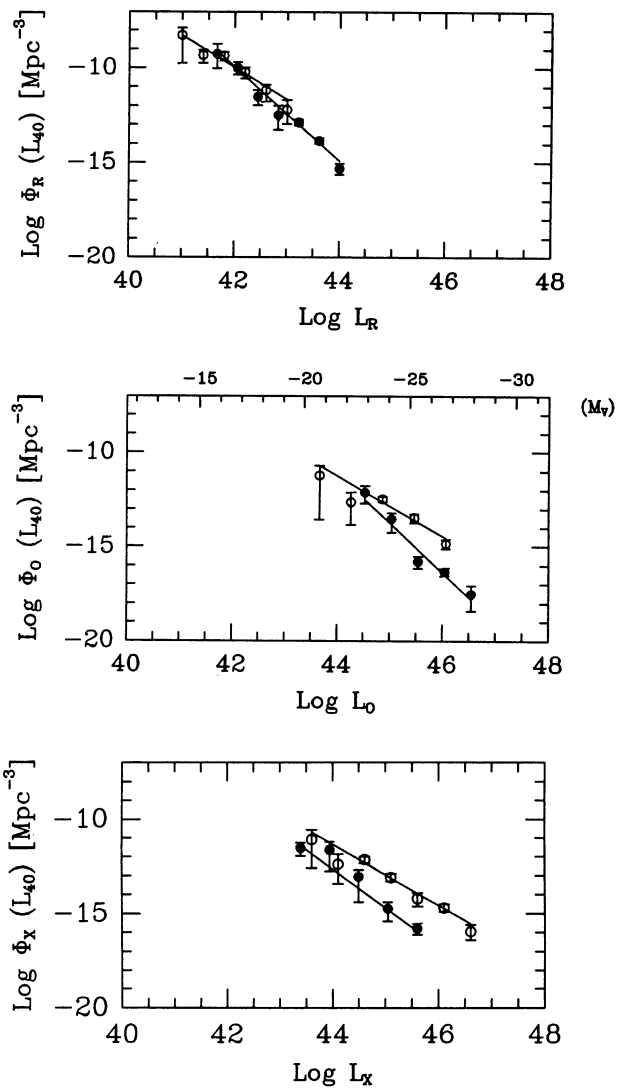

FIG. 2.—The computed de-evolved differential LFs for XBLs (*open circles*) and RBLs (*filled circles*). LFs are superposed for ease of comparison. (*From top to bottom*) Radio, optical and X-ray band. The scale is the same in the three panels. Luminosities are in erg's s^{-1}; densities are in Mpc^{-3} L_{40}^{-1}. In the optical panel, an axis with absolute magnitudes is plotted for ease of reference. Best-fit lines are derived from least-squares fits.

extreme values. We have found that, assuming a value of $z = 0.2$ (the minimum value possible) for these objects, the slopes of the radio and optical LFs increase ($B'_R = 2.62$, $B'_O = 3.08$), but the overall distribution remains within the errors. The slope of the X-ray LF does not change significantly. In the case of the X-ray LF we have also estimated the effect of including the five objects with unknown X-ray flux, computing the values of fluxes in the X-ray band on the basis of their optical and radio fluxes and their redshifts. The introduction of these objects does not change significantly the values of the slope ($B'_X = 2.02$) or of the normalization factor.

4. DISCUSSION

We have derived here for the first time the optical LF for two complete samples of BL Lac objects. We must regard in principle these two LFs as lower limits on the actual optical LF since radio-quiet and/or X-ray quiet BL Lacs may be found in

TABLE 4A

PARAMETERS AND VALUES FOR LFs IN THE THREE BANDS FOR XBLs

Parameter	Radio	Optical	X-ray
B	1.70 ± 0.26	1.60 ± 0.18	1.62 ± 0.13
$\log K$	-6.58 ± 0.49	-4.35 ± 0.94	-4.84 ± 0.70
χ^2 (dof)	4.29 (4)	7.26 (3)	5.84 (5)

NOTES.—K is in units of $\mathrm{Mpc}^{-3}\ L_{40}^{B-1}$, where L_{40} is the luminosity in units of 10^{40} ergs s^{-1}.

TABLE 4B

PARAMETERS AND VALUES FOR LFs IN THE THREE BANDS FOR RBLs

Parameter	Radio	Optical	X-ray
B'	2.48 ± 0.17	2.62 ± 0.28	1.99 ± 0.20
$\log K$	-5.00 ± 0.55	-0.63 ± 1.62	-4.63 ± 0.96
χ^2 (dof)	4.77 (5)	6.04 (3)	1.78 (3)

NOTES.—K is in units of $\mathrm{Mpc}^{-3}\ L_{40}^{B'-1}$, where L_{40} is the luminosity in units of 10^{40} ergs s^{-1}.

optical searches. However, from the results of Stocke et al. (1990) we know that radio-quiet BL Lac objects, if they indeed exist, are either a small fraction ($\sim 10^{-3}$) of radio-loud BL Lac objects or they are also X-ray quiet; furthermore, Ku (1980) and Schwartz & Ku (1980) have reported that a large fraction (consistent with unity) of all BL Lac objects known at the time are X-ray bright and do indeed exhibit X-ray luminosities roughly 10% or more of the optical luminosity. Thus we can interpret these LFs as valid estimates of the volume densities of BL Lac objects in the optical band.

Having derived the LFs for XBLs and RBLs, we want to compare them in the three bands, in order to define possible differences and analogies, and to match them against the predictions of current models. We will also compute the optical number counts ($\log N$-m).

4.1. *Comparison between XBL and RBL*

In Figure 2 we superpose the LF for the two samples in each band (radio, optical, X-ray). Differences are evident in all the three bands. In the X-ray and optical bands, the range of observed luminosities are very similar, and the XBLs have an higher volume density. In the radio band, instead, the densities are similar in the overlapping luminosity region, while the XBLs are found at lower luminosities than RBLs. We will try here to interpret these results within the general context of the beaming models. A more detailed approach to this comparison with models, for the case of minimal cosmological evolution, is presented in § 4.2. We recall that it has been suggested that the best way of explaining the overall properties of BL Lac objects is relativistic beaming. Many observed features (i.e., higher contribution from galactic starlight, lesser variability and lesser variable polarization for XBLs) suggest that XBLs are less beamed than RBLs (see, e.g., Stocke et al. 1990). If RBL and XBL densities are proportional to the solid angle subtended by the jet, a wider X-ray beam would explain the higher densities for XBLs (the ratio between XBLs and RBLs ranges in the X-ray from ~ 30 at 10^{44} ergs s^{-1} to ~ 130 at 10^{46} ergs s^{-1} and in the optical from $\gtrsim 1$ at 10^{44} ergs s^{-1} to ~ 80 at 10^{46} ergs s^{-1}). The steeper slope of the RBL LFs remains to be explained. In the radio band the densities are comparable at 10^{42} ergs s^{-1}, where the two functions overlap. The lower luminosity for XBLs could be due to the fact that, if the X-ray emission solid angle is larger, many lines of sight to an XBL lie outside the radio cone. In this picture, the radio emission as seen by us is not Doppler boosted, and hence fluxes are lower. This is consistent with the results obtained by Perlman & Stocke (1993) from a comparison of the radio properties of XBLs and RBLs. These authors found that, statistically, the core-to-extended radio flux ratios of the XBLs are intermediate between F-R I radio galaxies and RBLs, suggesting that the radio emission of the XBLs is less beamed with respect to the radio emission of the RBLs.

We recall that an essential role in determining the relative abundance of objects in the two classes is played by the evolution. While in the next section we consider a minimal evolution case (almost consistent with no evolution), a general model needs to take into account the observed evolution and to explain the discrepancy in the sign of the evolution found in the two samples. A decrease of the X-ray emitting angle over cosmic time is one way of explaining the observed lack of XBLs in the past.

4.2. *The Radio and X-Ray LFs: Constraints to the Models*

The most convincing interpretation of the emission of the BL Lac objects is still that given by Blandford & Rees (1978), which involves the effect of relativistic beaming from bulk motion of radiating plasma in a jet. It has been proposed that BL Lac objects are low-power radio galaxies, i.e., F-R I radio galaxies, seen at small angles with the axis of the radio jet. The best way of testing this model is to compare the spatial density of the BL Lac objects with that of the proposed parent population (the F-R I radio galaxies). In this framework, the differences observed in the samples of BL Lac objects selected at different wavelengths, i.e., in the radio and in the X-ray bands, are explained assuming that the radio power is emitted within a solid angle smaller than the X-ray one. In this way, the XBL are F-R I galaxies seen at angles that are, on average, larger than the radio ones, and thus the properties of these objects are less extreme. In a recent paper Maraschi, Celotti, & Ghisellini (1991) proposed a scheme to unify F-R I galaxies, XBLs, and RBLs, in which the different widths of the emission cones in the radio and X-ray band are due to a different collimation of the jet (the "wide jet" model, hereafter WJM). In this context, the velocity of the relativistic plasma is constant, while the solid angle subtended by the directions of motion is larger in the inner part (where the X-rays are emitted) than in the outer part (where the radio emission is produced).

Celotti et al. (1993), using the procedure described here to derive the observed LF, have analyzed the WJM in detail and tested against the data available in literature (i.e., the 22 XBL sample of Morris et al. 1991 and the 34 RBL sample of Stickel et al. 1991), by comparing directly the radio and the X-ray LFs of both XBLs and RBLs. From this comparison they were able to derive the following set of parameters: the X-ray radiation is emitted in a wider cone of width $\Theta_X = 13°$, and the radiation in the radio band is confined within a cone of width $\Theta_R = 2/\Gamma = 4°$ (Lorentz factor $\Gamma = 29$); the fraction of beamed luminosity of the moving plasma in the rest frame to unbeamed luminosity in the X-ray and radio bands is $f_X = 5 \times 10^{-3}$ and $f_R = 6 \times 10^{-3}$. As already noted in Celotti et al. (1993), the values of the parameters of the model critically depend on the assumptions on the evolution and are affected by the uncertainties on the observed LF.

Since we have significantly extended the sample of XBL and revised the X-ray evolution parameter, we can recompute the

radio and X-ray LFs for the XBLs under the same hypothesis as the Celotti et al. (1993) paper (i.e., using the minimal evolution compatible with the observed data) and plot them against the LF predicted by the WJM (see Fig. 3). For RBLs we have assumed a zero evolution both in the radio and in the X-ray band, while for the XBL a parameter $c_R = -0.7$ [$L(z) = L(0) \exp(c\tau)$] in the radio, a parameter $c_X = -1.3$ in the X-ray band, which are the minimum values in the 2 σ confidence range found with the V_e/V_a test (see § 3.2).

The new LFs are still consistent with the model; notably, the evidence of a break at low luminosities in the radio LF of XBLs is lessened with the new computation; on the other hand, the agreement with the predicted LF has improved ($\chi^2_3 = 1.1$ to be compared with $\chi^2_3 = 2.1$ relative to the sample of 22 XBLs).

In this paper, the X-ray LFs of both XBL and RBL is computed with an evolution parameter slightly lower than that used by Celotti et al. (1993). For this reason the LFs of the two samples have a lower normalization. A weighted least-squares fit with a fixed slope of $B = 2.1$ (the same as the parent population; see Celotti et al. 1993) gives a normalization of the X-ray LF of XBL of $\log K = -3.11 \pm 0.83$ Mpc^{-3} L_{40}^{B-1}, to be compared with the value of -2.85 ± 1.16 found with the sample of 22 XBLs. For the RBLs we find $\log K = -3.87 \pm 0.85$ Mpc^{-3} L_{40}^{B-1}, which, again, is fully consistent with the value of -3.49 ± 1.10 using the evolutionary values of Celotti et al. (1993).

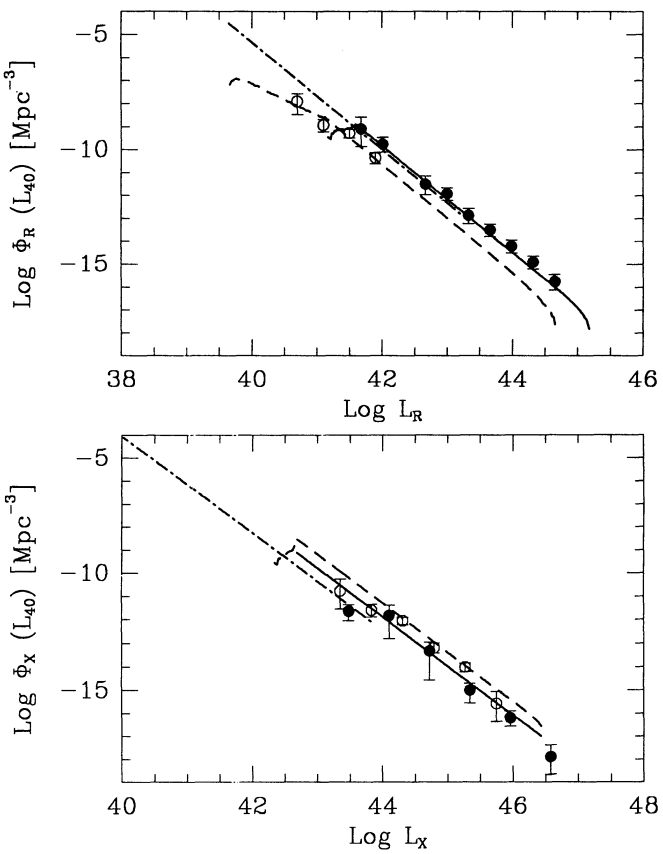

FIG. 3.—(*a*) The differential X-ray luminosity function of BL Lac objects calculated assuming F-R I radio galaxies as parent population (the LF of which is shown as *dot-dashed line*), for the parameters given in the text. The continuous and dashed lines represent the XBL and RBL LFs derived from the model, respectively. The LF (minimal evolution) of XBL (*open circles*) and RBL (*filled circles*) are also reported. (*b*) Same as (*a*), in the radio band. (Model from Celotti et al. 1993).

In conclusion, the agreement of the model with the observations is still good; nevertheless, a more substantial increase in the size of the complete samples of BL Lac objects is needed in order to reduce the errors on the observed LFs and to set more stringent constraints on the model.

An alternative scenario of unification for RBLs and XBLs is the one proposed by Giommi, Ansari, & Micol (1994), in which a single population exists, characterized by a similar radio to infrared energy distribution and a spread in energy cutoffs at higher energies. RBLs would make up the bulk of the population, while XBLs are those rare BL Lac objects in which the spectral break is at sufficiently high energy that the X-ray flux is above the survey limits. A prediction of the X-ray number counts expected using this model, the observed radio counts, and the probability distribution of having a given X-ray-to-radio flux ratio is given by Giommi & Padovani (1994) and found to agree with the observational data of various X-ray surveys.

4.3. *Optical Counts of BL Lacertae Objects*

As a result of the failure to find BL Lac objects through optical searches, the optical log N-m of BL Lacs is not known. Estimates of the surface density of these objects based on the available heterogeneous list of BL Lac objects have appeared in the literature (Padovani & Urry 1991). These estimates, however, are very uncertain: the optical samples used to constrain the resulting optical counts were not complete, and many hypotheses had to be made, yielding possible variations in the density at a given magnitude of about a factor of 10. We are in a position to compute a more reliable and accurate estimate of the visual log N-m of BL Lac objects by integrating the optical luminosity function derived in § 3.3. Since the beaming models imply that a fraction of XBLs are also RBLs, we will integrate the optical LFs of XBLs and RBLs separately.

The result is shown in Figure 4 and has been obtained integrating the LF of Figure 2*b* (*open circles*), taking into account its cosmological evolution (see Table 3A) from $M_{V_1} = -20.8$ ($L_{\rm min} = 5 \times 10^{43}$) to $M_{V_2} = -27.8$ ($L_{\rm max} = 3.2 \times 10^{46}$ ergs s^{-1}) and from $z_{\rm min} = 0$ to $z_{\rm max} = 3$ for XBLs (*a*), and integrating the LF of Figure 2*b* (*filled circles*) with the cosmological evolution from Table 3B, from $M_{V_1} = -22.3$ ($L_{\rm min} = 2 \times 10^{44}$) to $M_{V_2} = -28.3$ ($L_{\rm max} = 5.0 \times 10^{46}$ ergs s^{-1}) and from $z_{\rm min} = 0$ to $z_{\rm max} = 3$ for RBL (*b*). It should be noted that since we are interested in computing the space density of these objects over a magnitude interval ($m_V \sim 15$–20) reachable with current telescopes, the higher limit in the integration over redshift does not play a significant role. No XBLs, and ~20% of RBLs with $z > 1$ contribute in fact to the estimated counts, even at the faint end ($m_V = 20$) of the distribution. Only ~3% of RBLs are found at $z > 2$. Similarly, a minor role is played by the lower and upper limits of the integration over luminosities. For XBLs, when the fainter magnitude, M_{V_1}, is lowered from -20.8 to -19.6 the number of objects increases by ~10% (mainly at faint magnitudes), while an increase of ~30% (mainly at bright magnitudes) is seen when M_{V_2} is set to -28.1. For RBLs, the lower limit of integration plays a more important role, since the LF is steeper: the number density nearly doubles at low fluxes going about 1 mag fainter. At high fluxes, on the other hand, the variation is only of 5% for an increase of 1.3 mag in the integration limit. The uncertainty in the evolution parameter and in the slope of the LF has a marginal

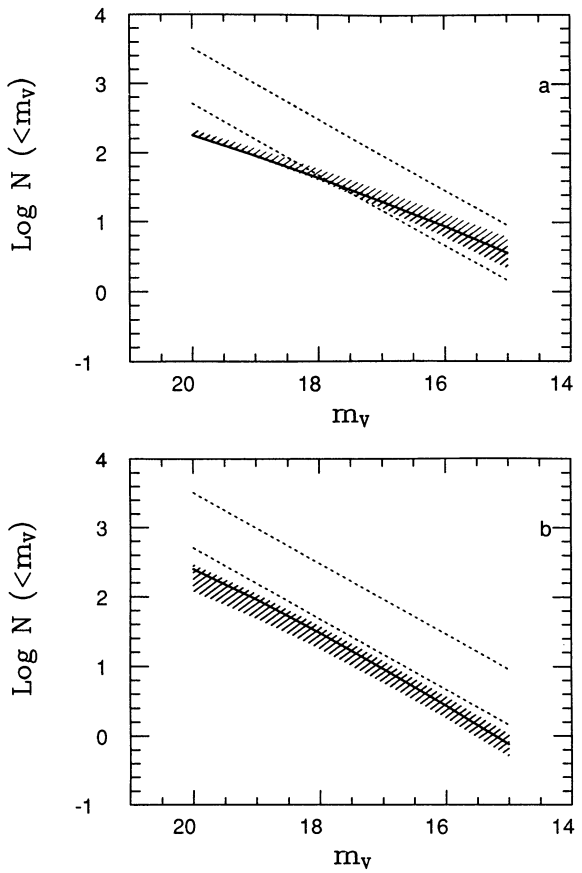

FIG. 4.—The log N-m derived from the integration of the (*a*) XBL optical LF and (*b*) RBL optical LF. The solid line represents the best estimate, while the shaded area indicates the possible variations of the densities introduced by the uncertainties on the evolution parameter and on the LF slope (see text for details). For reference, the range of densities computed by Padovani & Urry (1991) (*dotted lines*) is plotted.

impact on the result of the integration. Using the $\pm 1\ \sigma$ values on c_O and B_O, we have obtained deviations of $\lesssim 30\%$ with respect to the results obtained with the best-fit value. The shaded area in Figure 4 around the best-fit value (indicated by a continuous line) shows the variations in the optical counts resulting from the combined uncertainties in the evolution parameters and in the LF slope. The dominating effect in determining the range of the optical number counts is the uncertainty in the evolution parameter. The other parameters, even if not well determined, do not affect significantly the resulting number counts. The limits on the number counts derived by Padovani & Urry (1991) are plotted for reference.

At $m_V = 15.6$ (which corresponds, assuming an average $B-V = 0.6$, to the average limit of $m_B = 16.2$ of the Palomar-Green sample [Green et al. 1986]) the density of BL Lac objects is ≈ 6 per steradian. Thus, some 20 objects should be found in the PG sample which covers 10,714 deg^2 of sky at the $m_B = 16.2$ limit. Only three BL Lac objects were listed in the complete flux-limited sample of UV-excess objects in the PG survey. A recent paper (Fleming et al. 1993), however, doubles the number of BL Lac objects in the same sample, by identifying three previously misclassified DC white dwarfs with BL Lac objects. Hence, since only six BL Lac objects are found, out of the 20 expected, in the sample with $U-B < -0.44$, we can conclude that only $\sim 30\%$ of BL Lac objects show this UV excess. Indeed, the fact that not all BL Lac objects have blue optical spectra is evident from the EMSS BL Lac spectra published in Morris et al. (1991). To gather a sizable sample of objects (~ 100) of sufficiently bright magnitude to allow detailed spectroscopic studies ($m_V \sim 17.5$–18), one has to survey about 2 sr of sky, a challenging but feasible project.

Our results on the optical space density of BL Lac objects are consistent with the null result from polarization surveys (see Table 2 and Table 3 in Jannuzi et al. 1993a for the level of sensitivity to the polarization, usually larger than 5% and with uncertainties that depend on the magnitude of the object but are generally of the order of 5%–10%), given the average low polarization ($< 10\%$) of XBLs (Jannuzi et al. 1993b) and the duty cycle of polarized emission (fraction of time at a polarization degree greater than 4%) of 40% for XBLs (Jannuzi et al. 1994).

4.4. *The Problem of Recognition of BL Lacertae Objects at Low Redshifts*

In a recent paper Browne & Marcha (1993) outline the possibility that deep X-ray surveys may be affected by a bias introduced by the difficulty in recognizing low-luminosity BL Lac objects, since they lie in the nuclei of luminous elliptical galaxies, and suggest that this may result in an important selection effect on statistical studies based upon deep surveys. The authors point out that the selection of a sample of BL Lac objects is always made through optical criteria; when the difference in flux densities between the BL Lac object and the galaxy is small (typically 1 mag) it becomes impossible to recognize the BL Lac object as such. Browne & Marcha (1993) discuss the relevance of these misclassifications for different surveys, assuming that BL Lac objects as faint as $L_X \sim 2 \times 10^{39}$ ergs s^{-1} exist. They show that the effect begins to be relevant at fluxes less than 10^{-13} ergs cm^{-2} s^{-1} and becomes important for very deep surveys. For example, under certain hypotheses about the LF and the optical-to-X spectral index, it would be difficult to detect a BL Lac–type nucleus in an average elliptical galaxy at any redshift < 0.4, if the object has an X-ray flux near the limit of a survey with a flux limit of 4×10^{-9} Jy at 2 keV (corresponding to 5×10^{-14} ergs s^{-1} cm^{-2} in the 0.3–3.5 keV band, if $\alpha_X = 1$). They conclude, therefore, that the EMSS survey, which contains objects with flux densities as low as 4×10^{-9} Jy, suffers from misclassifications for redshift less than 0.4. We do not agree with these conclusions, as we explain below.

In Figure 5 we report the sky coverage of the EMSS, i.e., the fraction of sky covered by the survey as a function of the flux limit. The survey may be considered as the sum of different subsurveys, made at a given flux limit, all weighted by the fraction of the sky covered at that flux limit. In order to compute the effect of the recognition bias on the survey, we have to consider the incidence of the bias for each part of the survey, i.e., for the different flux limits, and weigh each contribution on the basis of the area covered at that flux. Figure 5 clearly shows that, although the EMSS reaches the flux limit of $\sim 5 \times 10^{-14}$ ergs cm^{-2} s^{-1}, only a very small area is covered at this flux and gives a marginal contribution to the source sample (only 2% of the sources have a flux $\leq 10^{-13}$ ergs cm^{-2} s^{-1} and only 17% a flux $\leq 2 \times 10^{-13}$ ergs cm^{-2} s^{-1}). For this reason, the effect of the possible misclassification in the EMSS should be computed at fluxes much higher than those used by Browne & Marcha (1993), where the effect of the bias is smaller.

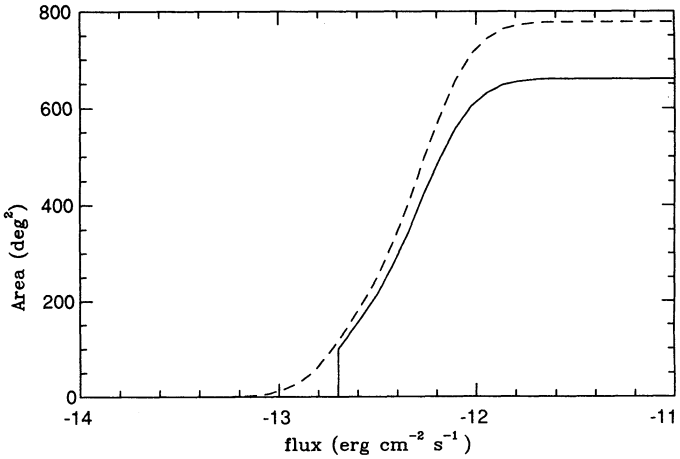

FIG. 5.—The sky coverage of the EMSS, fluxes in ergs cm^{-2} s^{-1}, areas in deg^2 (*dashed line*). The solid line represents the sky coverage used in this paper.

In conclusion, we believe that the recognition problem may apply—if indeed these low luminosity BL Lac objects exist—to much deeper surveys but not to the EMSS in general and certainly not to the sample used in this paper, which has a flux cutoff at 2×10^{-13} ergs cm^{-2} s^{-1}.

5. CONCLUSIONS

We use a complete sample of XBLs and a complete sample of RBLs to derive the LFs in the three bands: radio, optical, and X-ray. For the first time, we present an optical LF derived from a complete sample of BL Lac objects. We are then able to predict the surface density of BL Lac objects at different apparent magnitudes, and we find that commonly used optical search methods miss the large majority of BL Lac objects.

A reasonably sized region (~ 2 sr) has to be surveyed to find large (~ 100) samples of optically bright BL Lac objects. It has been demonstrated that combined X-ray and radio flux information allows the creation of samples that contain a large fraction of BL Lac objects (see, e.g., Stocke et al. 1990 and Schachter et al. 1993). However, it would be useful to devise a search method that is based solely on optical properties in order to produce an independent optically selected sample.

We have generalized the $1/V_a$ estimator of Avni & Bahcall (1980) to compute the LF in the nonselection band. From the comparison of the XBL and RBL LFs we find that XBLs greatly outnumber RBLs, up to a factor of more than 100 at high X-ray luminosities. XBLs and RBLs are found in about the same range of luminosities in the optical and X-ray band, while radio luminosities are significantly lower for XBLs. All these differences are well explained qualitatively by a model like the WJM (proposed by Maraschi et al. (1991) and tested against the data by Celotti et al. 1993), in which the radio cone is smaller than the X-ray one. The smaller solid angle needed to produce an RBL explains the smaller number of RBLs found; at the same time, the fact that XBLs are most probably seen from a direction that lies outside the radio cone means that radio luminosities are not Doppler boosted, and hence radio fluxes and luminosities are lower than RBL for comparable observed X-ray luminosities.

A theoretical model that takes into account and explains the different evolution found (negative for XBLs and positive for RBLs) is, however, needed.

We thank A. Celotti, R. Griffiths, P. Padovani, and the referee S. Morris for useful comments and discussions that helped improve the paper. We also thank P. Giommi for communicating results in advance of publication. This work has received partial financial support from the Italian Space Agency (ASI contract 92-RS-56) and from the European Economic Community (EEC contract ERB-CHRX-CT92-0033).

REFERENCES

Avni, Y., & Bahcall, J. N. 1980, ApJ, 235, 694
Biermann, P. L., Shaaf, R., Pietsch, W., Schmutzler, T., Witzel, A., & Kühr, H. 1992, A&AS, 96, 339
Blandford, R. D., & Rees, M. J. 1978, in Pittsburgh Conference on BL Lac Objects, ed. A. N. Wolfe (Pittsburgh: Pittsburgh Univ. Press), 328
Browne, I. W. A., & Marcha, M. J. M. 1993, MNRAS, 261, 795
Celotti, A., Maraschi, L., Ghisellini, G., Caccianiga, A., & Maccacaro, T. 1993, ApJ, 416, 118
Della Ceca, R., Maccacaro, T., Gioia, I. M., Wolter, A., & Stocke, J. T. 1992, ApJ, 389, 491
Falomo, R. 1991, AJ, 102, 1991
Fleming, T. A., Green, R. F., Jannuzi, B. T., Liebert, J., Smith, P. S., & Fink, H. 1993, AJ, 106, 1729
Gear, W. K. 1993, MNRAS, 264, 919
Gehrels, N. 1986, ApJ, 303, 336
Gioia, I. M., & Luppino, G. 1994, ApJS, in press
Gioia, I. M., Maccacaro, T., Schild, R. E., Wolter, A., Stocke, J. T., Morris, S. L., & Henry, J. P. 1990, ApJS, 72, 567
Giommi, P., Ansari, S. N., & Micol, A. 1994, A&A, submitted
Giommi, P., & Padovani, P. 1994, MNRAS, submitted
Green, R. F., Schmidt, M., & Liebert, J. 1986, ApJS, 61, 305
Hawkins, M. R. S., Veron, P., Hunstead, R. W., & Burgess, A. M. 1991, A&A, 248, 421
Isobe, T., Feigelson, E. D., Akritas, M. G., & Babu, G. J. 1990, ApJ, 364, 104
Jannuzi, B. T. 1990, Ph.D. thesis, Univ. of Arizona
Jannuzi, B. T., Green, R. F., & French H. 1993a, ApJ, 404, 100
Jannuzi, B. T., Smith, P. S., & Elston, R. 1993b, ApJS, 85, 265
———. 1994, ApJ, 428, 130
Ku, W. H.-M. 1980, in Highlights of Astronomy, Vol. 5, ed. P. A. Wayman (Dordrecht: Reidel), 677
Kühr, H., Witzel, A., Pauliny-Toth, I. I. K., & Nauber, U. 1981, A&AS, 45, 367
Laurent-Muehleisen, S. A., Koolgaard, R. I., Moellenbrock, G. A., & Feigelson, E. D. 1993, AJ, 106, 875
Maccacaro, T., Della Ceca, R., Gioia, I. M., Morris, S. L., Stocke, J. T., & Wolter, A. 1991, ApJ, 374, 117
Maccacaro, T., Gioia, I. M., Wolter, A., Zamorani, G., & Stocke, J. T. 1988, ApJ, 326, 680
Maraschi, L., Celotti, A., & Ghisellini, G. 1991, in The Physics of Active Galactic Nuclei, ed. W. J. Duschl & S. I. Wagner (Berlin: Springer-Verlag), 605
Maraschi, L., Ghisellini, G., Tanzi, E., & Treves, A. 1986, ApJ, 310, 325
Marshall, H. T. 1985, ApJ, 299, 109
Morris, S. L., Stocke, J. T., Gioia, I. M., Schild, R. E., Wolter, A., Maccacaro, T., & Della Ceca, R. 1991, ApJ, 380, 49
Padovani, P. 1992, A&A, 256, 399
Padovani, P., & Urry, C. M. 1990, ApJ, 356, 75
———. 1991, ApJ, 368, 373
———. 1992, ApJ, 387, 449
Perlman, E. S., & Stocke, J. T. 1993, ApJ, 406, 430
Schachter, J. F., et al. 1993, ApJ, 412, 541
Schneider, D. P., Schmidt, M., & Gunn, J. E. 1991, AJ, 101, 2004
Schwartz, D. A., & Ku, W. H.-M. 1980, BAAS, 12, 873
Stickel, M., Padovani, P., Urry, C. M., Fried, J. W., & Kühr, H. 1991, ApJ, 374, 431
Stocke, J. T., Liebert, J., Schmidt, G., Gioia, I. M., Maccacaro, T., Schild, R., Maccagni, D., & Arp, H. 1985, ApJ, 298, 619
Stocke, J. T., Morris, S. L., Gioia, I. M., Maccacaro, T., Schild, R. E., & Wolter, A. 1989, in BL Lac Objects, Vol. 334, ed. L. Maraschi, T. Maccacaro, & M.-H. Ulrich (Berlin: Springer-Verlag), 242
———. 1990, ApJ, 384, 141
Stocke, J. T., Morris, S. L., Gioia, I. M., Maccacaro, T., Schild, R. E., Wolter, A., Fleming, T. A., & Henry, J. P. 1991, ApJS, 76, 813
Urry, C. M., Padovani, P., & Stickel, M. 1991, ApJ, 382, 501